Theory of the structural and electronic properties of α-Ga(001) and (010) surfaces

M. Bernasconi* and Guido L. Chiarotti
International School for Advanced Studies, Via Beirut 2, I-34014 Trieste, Italy

E. Tosatti
International School for Advanced Studies, Via Beirut 2, I-34014 Trieste, Italy
and International Center for Theoretical Physics, P.O. Box 586, I-34014 Trieste, Italy
(Received 9 August 1994; revised manuscript received 22 March 1995)

We present a comprehensive study of the (001) and (010) surfaces of α-Ga via *ab-initio* local density calculations. Based on this it is predicted that the (001) surface should be covered in the ground state by two layers of epitaxial GaIII, a denser phase stable in the bulk at high pressures and temperatures. On the contrary the ground state of the (010) surface is found to be unreconstructed. For both surfaces, we present the calculation of the band structure. Features related to the presence or absence of reconstruction are pointed out. A comparison with existing scanning tunneling microscope data is given.

I. INTRODUCTION

Gallium is one of few metals that do not crystallize in any of the simple crystal structures. The stable phase at normal conditions, α-Ga, is based centered orthorhombic with eight atoms in the conventional unit cell.[1] Gallium also possess a rather complicated phase diagram with many stable and metastable crystalline phases all closely competing for the ground state. Two phases, GaII and GaIII,[2] are stable at high pressure. In addition a number of metastable phases has been identified at atmospheric pressure designated β,[3] γ,[4] δ,[5] and ϵ.[2]

A peculiar feature of the α phase is that each atom has only one nearest neighbor in the first coordination shell centered at 2.44 Å, and six other neighbors within 0.39 Å further apart. The structure of α-Ga can be regarded as consisting of strongly buckled planes orthogonal to the c axis connected by short bonds between the first neighbors, which lie in different planes (see Fig. 1). A variety of experimental data—summarized in Ref. 6—reveal the partial covalent character of the short bonds, which can be seen to form essentially covalent Ga_2 dimers. There is a long history to the literature and ideas relating to covalency in α-Ga.[7,8] The covalency of the dimer and its fingerprint in the electronic properties, in particular the presence of a pseudogap at the Fermi level in the electronic densities of states, has recently been confirmed by first-principles calculations by Gong *et al.*[6], Hafner and Jank,[9] and by Bernasconi, Chiarotti, and Tosatti.[10] The double nature—covalent and metallic—of bulk α-Ga makes its surfaces especially interesting. The rule for *sp*-metal surfaces is not to reconstruct, while reconstruction is the rule for semiconductors, where bulk covalency forces the presence of unsaturated dangling bonds. Therefore, it is interesting to ask which of the two characters of α-Ga prevails on the different surface orientations.

Gallium has a very low melting temperature ($T_m = 303$ K) and a low vapor pressure at melting, which makes it a suitable system for the study of surfaces even very near T_m. In particular, theoretical arguments suggest that the surface of α-Ga should display either nonmelting or incomplete (blocked) surface melting.[11,12] This comes from the presence of attractive Van der Waals forces between the liquid surface and the liquid-solid interface of solid gallium wetted by a thick liquid film.[11]

These and other considerations have stimulated an extensive recent scanning tunneling microscope (STM) study of the α-Ga surfaces by Züger and Dürig.[13,14] It turns out that most α-Ga surfaces not only do not melt[15] but also display a very unusual and remarkable thermal stability. For instance, on the (001) and (010) surfaces neither step diffusion nor any other kind of surface mobility was detected up to T_m. Some of this apparent stability may just be due to insufficient diffusion at room temperature. Because of high diffusion barriers, the surfaces might still be out of equilibrium when bulk melting takes place. Even more surprisingly, the (001) surface is flat and atomically ordered, even when macroscopic amounts of the underlying bulk are already molten.[14] Despite these STM studies, the microscopic state of these surfaces, including detailed structure, electronic states, etc., is still largely unknown. We have, therefore, studied both the (001) and (010) surfaces within standard total-energy framework. In previous letters[16,17] we briefly reported our results on the structural properties of the (001) surface. We found that in one of the two possible ideal configurations of the (001) surface the covalent character of bulk α-Ga induces half-filled bands of surface dangling bonds. As in most semiconductors, the presence of unsaturated dangling bonds produces an instability, removed by a large rearrangement of surface geometry. Based on *ab-initio* calculation, we have proposed that in the ground state the (001) surface of α-Ga is covered by two layers of GaIII, a denser phase stable in the bulk only at high pressure and temperature. This self-wetting phenomenon is favored because the surface energy of the fully metallic GaIII is too much lower than the surface energy of the ideal relaxed α-Ga surface to make it worthwhile paying for interface energy plus the difference in bulk energy between α-Ga and GaIII, which is indeed very small. At

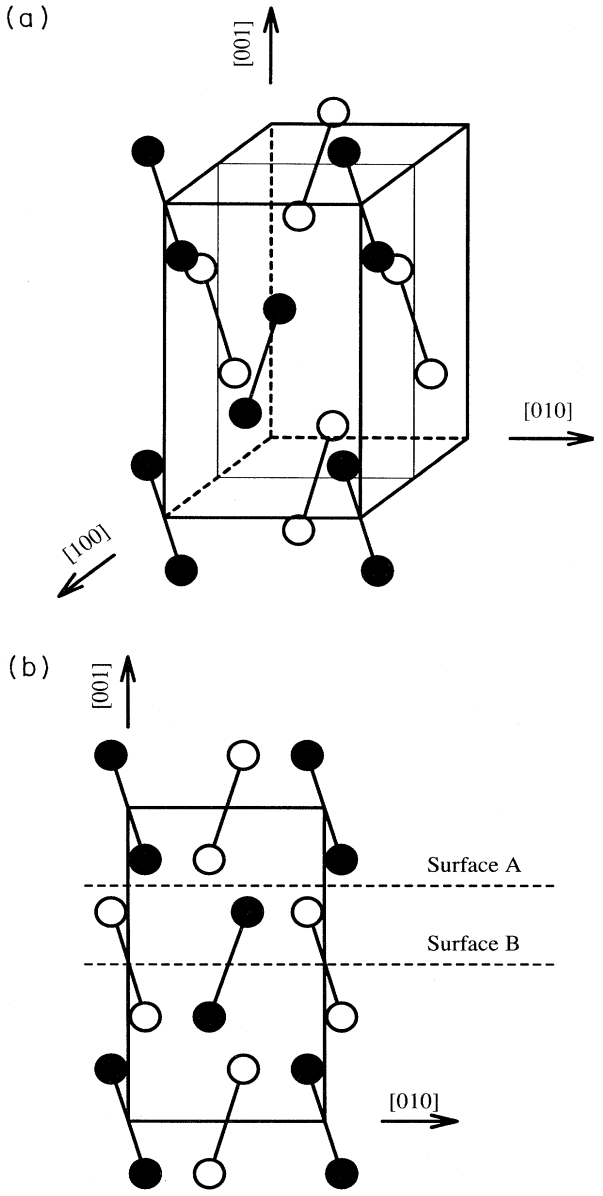

FIG. 1. (a) Orthorhombic unit cell of α-Ga. (b) Side view on the (100) plane. The solid circles represent atoms lying on the (100) plane at $x=a$, while the open circles atoms lie on the next lower plane at a depth of $x=a/2$. Atoms on the (100) plane at $x=0$ are in the same configuration of atoms at $x=a$ and are not reported. All dimers lie within the (100) planes. A and B indicate two inequivalent (001) surfaces, obtained by simple bulk cuts.

the atomic density of the thin film covering α-Ga, GaIII is known to melt 100 K above the melting point of α-Ga, probably accounting for the anomalous thermal stability of (001) surface.

In this paper we enlarge our scope and discuss, first of all, the electronic properties of the (001) surface in Sec. III. Surface-state bands are predicted in the stable surface configuration. Fresh results on the (010) surface are then discussed in Sec. IV. On this surface no covalent bonds are broken, and so no unsaturated dangling bonds are present to drive a surface reconstruction. As a result, atoms on the (010) orientation undergo only a minor rearrangement consisting of a 14° rotation of the surface Ga_2 dimers. Section V will be devoted to a general discussion and to conclusions.

II. COMPUTATIONAL METHOD

We studied structural and electronic properties of α-Ga surfaces within the *ab-initio* total-energy framework. We used standard density functional theory in the local-density approximation. For local exchange and correlation energy we adopted the parametrization of Perdew and Zunger.[18] An *ab-initio* norm-conserving pseudopotential for Ga was taken in the Kleinman-Bylander form,[19] constructed from the tables of Stupf, Gonze, and Scheffler.[20] Kohn-Sham (KS) orbitals were expanded in plane waves up to 14 Ry energy cutoff. Within this framework we have previously studied the structural and electronic properties of the bulk phases of gallium.[10] Lattice constants and internal structural parameters were optimized for bulk α-Ga, β-Ga, GaII, and GaIII, using Hellmann-Feynman forces[21] and stress.[22] High-precision Brillouin-zone (BZ) integrations[23] were performed using up to 300 k points in the irreducible Brillouin zone for the more metallic phases (27 are sufficient for α-Ga). The equilibrium energies and volumes per atom of α-Ga, β-Ga, GaII, and GaIII are, respectively, -4.5128, -4.5094, -4.5085, and -4.5075 Ry and 119, 111, 109, and 109 bohrs^3.[10]

In the present work, α-Ga surfaces have been modeled by periodically repeated slabs. (When not otherwise specified, the two surfaces of the slab are identical.) We used 14 layers for the (001) surface and 16 layers for the (010) surface. Convergence of k sums has been tested up to 49 k points in the irreducible ideal surface BZ (ISBZ); simple Gaussian spreading with variance from 20 to 5 mRy has been used.[24] Guided by the calculated Hellmann-Feynman forces we let all atoms in the slab relax to their lowest-energy positions, with residual forces less than 1.5×10^{-3} Ry/a_0. For the calculation of surface energies, we evaluated the bulk energy, to be subtracted from the total energy of the slab, by using a sampling grid in the surface plane identical to that used in the surface calculation and, perpendicular to the surface, equivalent to a slab thickness as close as possible to that used in the surface calculation. A one-to-one correspondence between the mesh of the bulk and the mesh of the slab is not always possible because in some cases the slabs used are not an integer number of bulk unit cells along the direction normal to the surface.

Surface stress calculation. In the slab calculation the in-plane lattice parameters are fixed to the equilibrium values obtained from the bulk calculation. On the assumption that the deep bulk portion of the slab is stress free, one can deduce the surface stress tensor from the stress tensor of the full three-dimensional (3D) slab supercell as

$$\sigma_{ij}^{\text{surf}} = -\partial\gamma/\partial\epsilon_{ij} = \tfrac{1}{2} d\,\sigma_{ij}^{\text{slab}} , \quad (1)$$

where d is the dimension of the supercell along the direction perpendicular to the surface, and i,j run over the surface coordinates. The surface stress was obtained from Eq. (1) with some important precautions. First, the stress calculated in the bulk from the wave functions through the stress theorem[22] is not zero at the minimum of the energy versus volume curve $[E(V)]$ calculated at constant cutoff (E_{cut}). This is a "basis set effect," which occurs because the stress derived from the stress theorem is computed with the number of plane waves held constant, while the derivatives of the curve $E(V)$ are calculated at constant E_{cut}. The difference between the stress at constant E_{cut} and at a constant number of plane waves is called the Pulay stress.[25] With our $E_{\text{cut}} = 14$ Ry, σ_{Pulay} at the bulk equilibrium volume of α-Ga is 3 kbar. This small value independently confirms the good convergence of our results with respect to E_{cut}. Second, even at the (bulk) equilibrium lattice parameter, the anisotropic part of the bulk stress is not zero if one uses a k-point mesh equivalent to the slab geometry instead of the bulk-converged k-point mesh. Thus for such a slab calculation the bulk stress is not zero, being the sum of this residual anisotropic stress, due to the k-point effect and σ_{Pulay}. To be consistent with our assumption that the bulk portion of the slab is stress free, this contribution must be subtracted from σ^{slab} in Eq. (1). In conclusion, we take

$$\sigma_{ij}^{\text{surf}} = \tfrac{1}{2} d \left[\sigma^{\text{slab}} + \frac{N}{V|_{\text{slab}}} \frac{V}{N|_{\text{bulk}}} (\sigma^{\text{bulk}}) \right] , \quad (2)$$

where σ^{bulk} is the stress obtained from a bulk calculation with the k mesh equivalent to the slab geometry. With these precautions, the stress perpendicular to the surface is indeed very close to zero (~ 0.5 kbar).

III. THE α-Ga(001) SURFACE

A. Surface structure

The (001) surface is the main stable surface of α-Ga with the highest packing density. It appears spontaneously on the crystal. The structure of the α-Ga(001) surface has been recently investigated by STM,[13,14] where it appears to be exceptionally stable: no step diffusion or other type of surface mobility was detected up to the bulk melting point ($T_m = 303$ K). More surprisingly, at T_m the Ga crystal begins to melt from *inside* the sample, with the surface still appearing flat, and atomically ordered.[14] By cooling the sample to room temperature just after the onset of bulk melting, large hillocks, emerging out from an otherwise flat (001) surface are observed by STM.[14] They are parts of micrometer-size droplets solidified after cooling below T_m. The area around the hillock is still in its original, atomically flat state. Obviously the liquid does not wet the (001) surface. The droplets forming the hillock structure have emerged from a melt in the underlying bulk. From the fact that atomically flat regions coexisted with a macroscopic liquid droplet on the surface, Züger and Dürig concluded[14] that the (001) surface was still stable when part of the underlying sample had already undergone the melting transitions.

Besides this rather anomalous thermal behavior, this surface raises additional questions. In principle, in fact, the ideal α-Ga(001) surface can be formed in two ways, by cutting the crystal at (a) a plane that separates dimer layers, without cutting "covalent" bonds (surface A) or at (b) a plane that cuts the dimer covalent bonds (surface B) (see Fig. 1). The top-view geometries for the ideal surfaces A and B are the same and can be described by a nearly square lattice with two atoms per surface cell, forming chains along the [100] direction, with coordinates (in lattice units) (0,0,0) and (0.5,0.34,0). The STM map clearly shows this chain structure.[13] Close inspection of the STM image also reveals a dimerization reconstruction. Locating the surface atoms at the maxima of the current spots in the image, Züger and Dürig assigned to the atom at the center of the cell a shift of ~ 0.35 Å, from the ideal position (0.5,0.34) to (0.45,0.4). They also suggested an ~ 0.05-Å buckling of the two atoms. The dimerization of the chain is independently supported by the static low-energy electron-diffraction (LEED) measurements which show a nonzero intensity of the spots $(2n+1,0)$ (in the surface notation), where n is an integer.[13] These spots have zero intensity in the ideal geometry because of the presence of the (100) mirror plane and will become nonzero because of either dimerization or buckling. Another feature revealed by STM is that surface steps on α-Ga(001) are of *diatomic* height $c/2 \simeq 3.8$ Å. If both configurations A and B were simultaneously realized, for example in adjacent domains, then steps with a height of $c/4 \simeq 1.9$ Å should be present at the domain boundaries; conversely, if one of the two surfaces had a much lower energy, the smallest step height expected would be $c/2 \simeq 3.8$ Å as observed. However, this still does not distinguish between possibilities A, B, and others. We studied in Refs. 16 and 17 both surfaces A and B and found that neither of the fully relaxed A and B configurations is favored. Both A and B surfaces end up having the same, rather high, surface energy ($\gamma_A \sim \gamma_B = 57$ mRy/atom, against $\gamma_{\text{expt}} \sim 41$ mRy/atom). However, a drastic rearrangement of surface geometry was found to produce a dramatic lowering of surface energy down to 47 mRy/atom. The final surface structure is shown in Fig. 2 and named surface C, and, remarkably, its top-view geometry is still similar to the ideal surface. In particular, the chains along the [100] direction still survive, and, in fact, our theoretical STM image reproduces the experimental STM data very well,[16] except for the chain dimerization and the buckling (which appear to be minor corrections with respect to our proposed massive atomic rearrangement) absent in our configuration.[26] The structure of the two outermost surface layers of surface C and their optimal charge density have become very reminiscent of those of bulk GaIII [see Fig. 2(a)]. Bulk GaIII is a tetragonally distorted fcc structure, stable at high pressure and temperature.[2,10] Here, it appears to wet the α-Ga(001) epitaxially. Actually, the chain structure at surface C is not present in the geometry of unstrained GaIII. However, we have checked that, by forcing bulk GaIII to have the same *in-plane* lattice constants as required by perfect epitaxy on α-Ga, its original fcc-

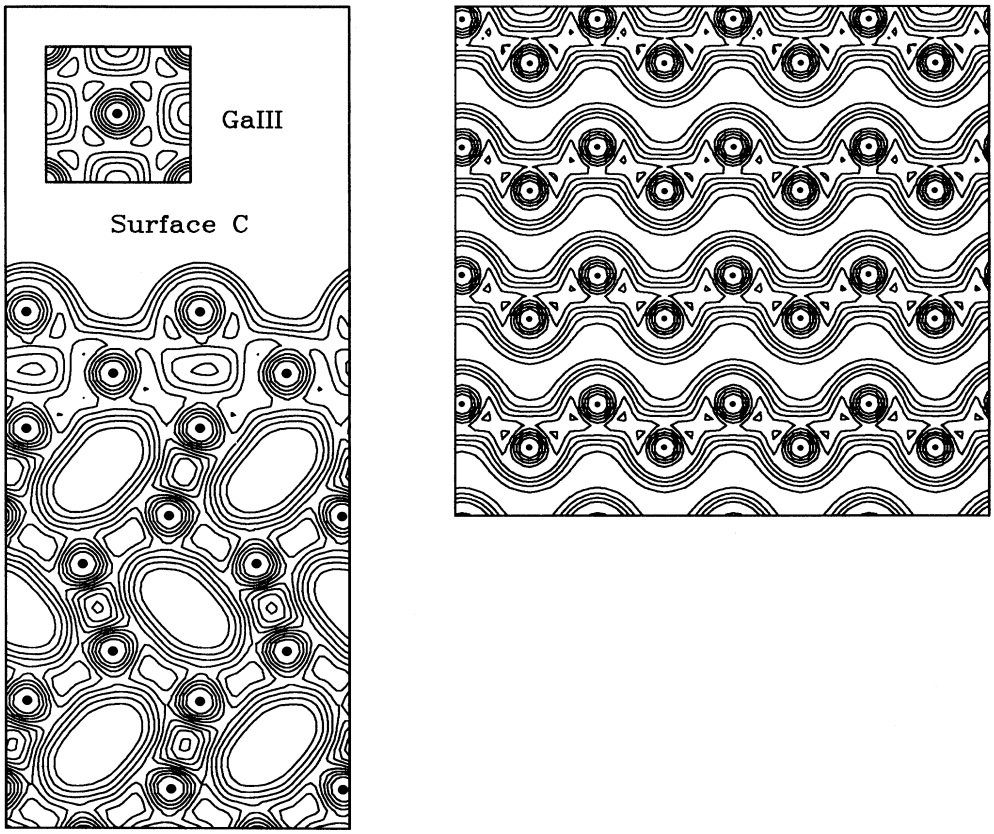

FIG. 2. Left panel: charge density of our proposed optimal structure for α-Ga(001) (surface C): $\gamma_C = 47$ mRy/atom. The fully relaxed interlayer distance for the outermost layers d_{12}, d_{23}, and d_{34} are 0.380, 0.347, and 0.525, respectively, in units of $a = 4.377$ Å. The corresponding (x,y) in-plane coordinates (in units of a) of the two atoms per cell in the four outermost planes are (0,0) (0.5, −0.324); (0,0.505)(0.5,0.171); (0,0.002)(0.5,−0.326); and (0,0.179)(0.5,−0.502), respectively. The two outermost surface layers now closely mimic the bulk GaIII phase (inset). Right panel: charge density of surface C plotted onto the surface plane (001). Contour lines are separated by 0.005 a.u.

like symmetry is unstable and the chain structure also appears in the bulk. This surface structure thus mimics GaIII epitaxially grown on α-Ga and will be referred to as "epitaxial GaIII." A separate study (made with a 12-layer slab) of the free surface of epitaxial GaIII gives rise to a top-layer structure, which is identical to that of our surface C.[27] We also find that the surface energy of epitaxial GaIII ($\gamma_{\rm III}$) is 43 mRy/atom. This value is sufficiently lower than the surface energy of the ideal configurations ($\gamma_A = \gamma_B = 57$ mRy/atom) to make it worth paying for an additional α-Ga/GaIII interface plus the difference in bulk energies of α-Ga and epitaxial GaIII [$\Delta E = E_{\rm bulk}$ (epitaxial GaIII) $- E_{\rm bulk}(\alpha$-Ga)], which we have separately calculated to be $\Delta E \sim 5$ mRy/atom. All these results support the prediction that in the ground state the (001) surface of α-Ga should be wetted by two layers of GaIII epitaxially grown on α-Ga. This prediction is now open for direct experimental verification. We also calculated the surface stress tensor, which was found to be tensile for surface C: $-\partial\gamma/\partial\epsilon_{xx} = -18$ mRy/atom and $-\partial\gamma/\partial\epsilon_{yy} = -50$ mRy/atom. (x and y are the [100] and the [010] directions in Fig. 2, and ϵ_{ij} is the strain.[28] The "k-point correction" discussed in Sec. II is included and equal to -22 mRy/atom, and -2 mRy/atom for $-\partial\gamma/\partial\epsilon_{xx}$ and $-\partial\gamma/\partial\epsilon_{yy}$, respectively.) The presence of a negative surface stress is obviously connected with the lateral expansion required for the structure of GaIII to fit epitaxially on α-Ga, with the associated contraction in the vertical in the vertical direction.

Once wetting has begun, one might perhaps expect the number of GaIII layers to grow. However, since adding a third GaIII layer produces a step height roughly one half the experimental value, the wetting must, in fact, be confined to the first two layers up to T_m, in order to be consistent with the surface morphology, as observed with STM. Indeed, by a separate calculation, we find that the surface energy of the relaxed configuration with *three* layers of GaIII (γ_3) is as high as 60 mRy/atom and that with *four* GaIII layers is $\gamma_4 = 65$ mRy/atom.[29] These values, compared with that of surface C ($\gamma_C = 47$ mRy/atom), guarantee that surface domains with one

and two, or with two and three GaIII layers are unlikely to be simultaneously present, in agreement with the observed step height distribution. Furthermore, the surface energy for three GaIII layers is much higher than the value obtained by adding to γ_C the bulk energy difference ΔE, required by the added GaIII plane.

We may write the overall surface energy of the configuration with n layers of GaIII on top of α-Ga as a sum of physically distinct terms

$$\gamma_n = \gamma_{\mathrm{III}} + \gamma_{\alpha\text{-III}} + n\Delta E + V(n) \tag{3}$$

where $\gamma_{\alpha\text{-III}}$ is the unperturbed interface energy (as obtained in the limit $n \to \infty$), and $V(n)$ is a surface-interface interaction potential.

From direct calculation, we know γ_{III} and ΔE, while $\gamma_{\alpha\text{-III}}$, and $V(n)$ are still unknown. Since $\gamma_4 - \gamma_3 \sim \Delta E$, we may assume $V(n)$ to be negligible for $n \geq 4$. Under this assumption the interface energy $\gamma_{\alpha\text{-III}}$ can be obtained from Eq. (3), and from the known quantities γ_4, γ_{III}, and ΔE as $\gamma_{\alpha\text{-III}} = \gamma_4 - \gamma_{\mathrm{III}} - 4\Delta E \simeq 2$ mRy/atom. From Eq. (3) and this estimated value of $\gamma_{\alpha\text{-III}}$ we can now also deduce the interaction energy $V(n)$. We find $V(2) \simeq -9$ and $V(3) \simeq -1$ mRy/atom, respectively for the $n = 2$ (surface C), and 3 GaIII layers. In Fig. 3 we plot the calculated surface energies as a function of covering GaIII layers and the "ideal" (asymptotic) surface energy for large n, when $V(n) \sim 0$. The difference between the ideal surface energy and the curve interpolating the surface energies is thus $V(n)$. As is evident from the figure, the surface-interface interaction is strongly *attractive* and limits the wetting film thickness to strictly two atomic layers, causing the wetting of α-Ga by epitaxial GaIII to be incomplete. The surface energy balance described above raises two puzzling equations, namely, why is $\gamma_{\alpha\text{-III}}$ so small, and why is $V(n)$ so attractive? The interface energy could be roughly expected to be a substantial fraction of the overall surface energies because of the difference in density of the two phases ($\sim 10\%$). An attraction between α-Ga and the GaIII-like surface is also unexpected, since the two lattices are very different, and spontaneous epitaxy is correspondingly difficult. This attraction is not associated with a visible dependence of the local atomic structure of the interface on the film thickness. In fact, we have calculated the interplanar distances for the configurations with different numbers of GaIII layers (Table I) and found a nearly constant interface structure (d_I and d_{dimer} in Table I). The origin of both the smallness of $\gamma_{\alpha\text{-III}}$ and the surface-interface attraction should therefore have a more subtle electronic origin. The distinguishing feature of GaIII is its unmitigated metallicity, as opposed to the semimetallicity of α-Ga. In Ref. 17 we have discussed how this surface "metallization" might precisely be the key to understand both the above questions. The interface energy is reduced by the charge transfer across the α-Ga–GaIII interface connected with an ~ 1-eV contact potential between the more electronegative α-Ga and more metallic GaIII. Furthermore, the source of the strong attraction between the GaIII/vacuum surface and the α-Ga/GaIII interface has been attributed to the short-range exchange-correlation forces. Their long-range part is known to be attractive for a good metal film on a poor metal substrate (negative Hamaker constant).[17] This attractive $V(n)$ compresses the thin GaIII film in surface C, producing a 3D atomic density roughly 8% higher than the bulk equilibrium density of epitaxial GaIII. If this density increase were obtained by hydrostatic pressure, it would cause GaIII to melt about 100 K above the melting temperature of α-Ga.[30] We have suggested that this finding could account for the anomalous thermal stability of the α-Ga(001) surface detected experimentally.[13,14] The next step, after the above characterization of the surface geometry and energetics, is a study of the surface electronic properties.

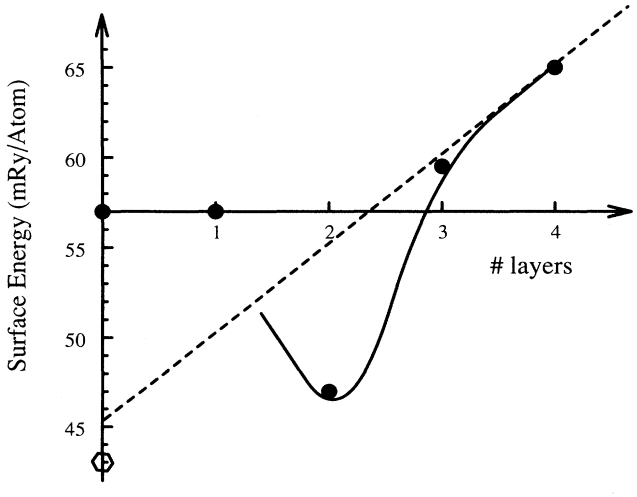

FIG. 3. Surface energies vs GaIII layers covering (see text). The values $n = 0$, 1, and 2 are those of surfaces A, B, and C, respectively. The empty hexagon represents the energy of the epitaxial GaIII surface. The dashed line represents the "ideal" surface energy (see text).

TABLE I. Interplanar distances of the outermost surface layers for configurations with 2, 3, 4, and ∞ numbers of GaIII layers epitaxially grown on α-Ga. The distances are in lattice units ($a = 4.38$ Å). d_I corresponds to the interplanar distance between the innermost GaIII layer of the film and the outermost dimer of α-Ga. d_{dimer} is the bond length of the outermost dimer of α-Ga. Note that both d_I and d_{dimer}, i.e., the interface structure, are poorly dependent on the thickness of GaIII film. $d = 0.398a$ in bulk epitaxial GaIII, and $d_{\mathrm{dimer}} = 0.528a$ in bulk α-Ga.

	$\alpha+2$ (C)	$\alpha+3$	$\alpha+4$	∞ (GaIII)
d_{12}	0.380	0.344	0.357	0.361
d_{23}		0.396	0.397	0.392
d_{34}			0.400	0.404
d_I	0.347	0.346	0.340	
d_{dimer}	0.525	0.526	0.529	

B. Band structure and electronic densities of states

The slab band structure of surface C along the high symmetry lines of the ISBZ is reported in Fig. 4. Before

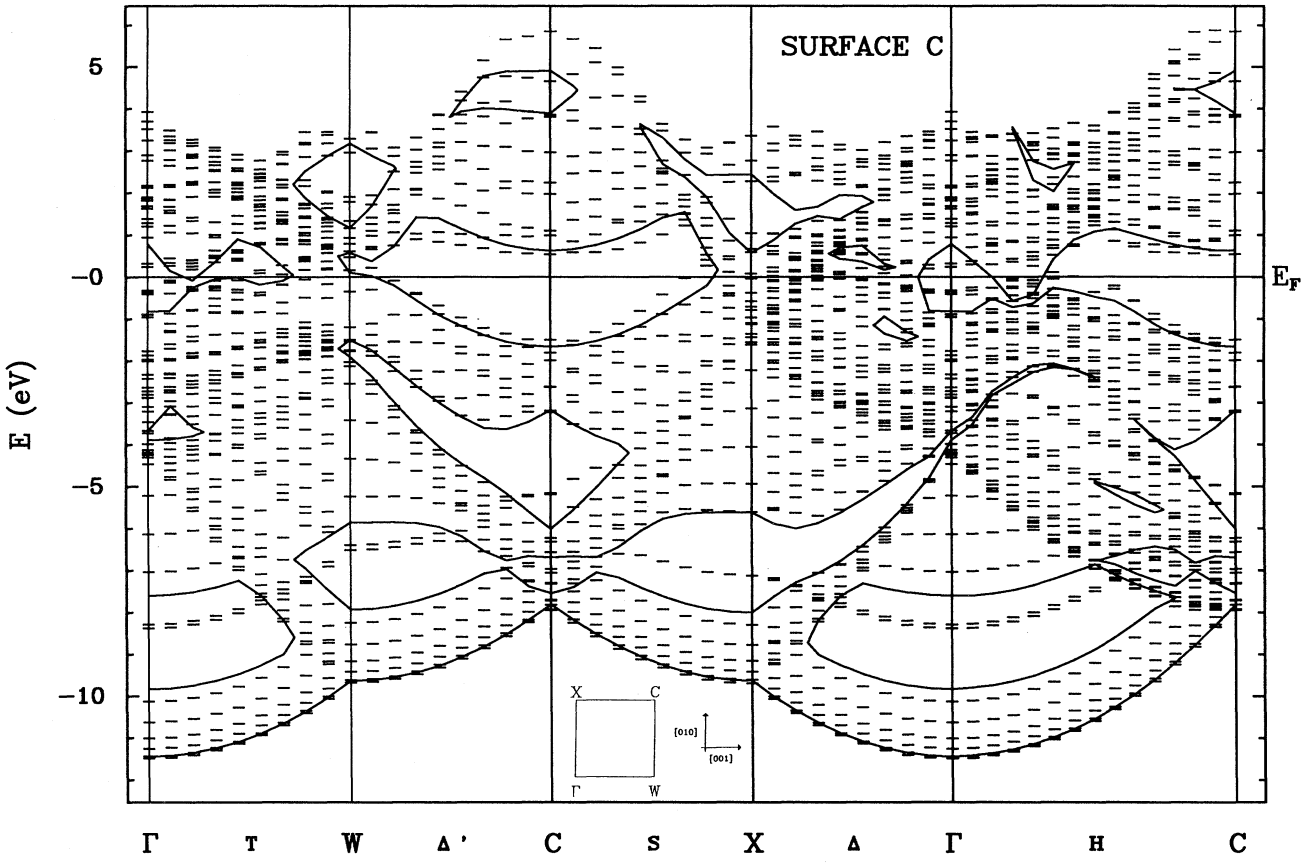

FIG. 4. The surface band structure of configuration C from a 14-layer slab. Continuous lines represent the band edges of the surface-projected band structure of the bulk. The zero in energy corresponds to the Fermi level. The energies of bulk and slab calculations are aligned by matching the average Hartree potential in the bulk and at the center of the slab. Inset: the irreducible surface Brillouin zone.

discussing it in detail, we show, for contrast, in Fig. 5 the band structure of the hypothetically ideal surface B (with truncated dimers). Well-defined surface states in the surface-projected bulk gap along S and Δ' directions crossing the Fermi level are present in surface B. These surface states correspond qualitatively to half-filled bands of surface *dangling bonds,* produced by the cutting off the outermost Ga_2 dimer. The two bands, split by the surface-surface interaction across the slab, are both double degenerate: there is one dangling bond per atom in the surface unit cell. Each dangling bond is strongly localized on one of the atoms in the surface unit cell, as is evident in Fig. 6. The two dangling bonds on different sublattices do not couple; they always point in opposite directions. They still "repel" each other if we artificially dimerize the chain along the [100] direction.[31] Thus, surface B cannot be stabilized by the formation of filled bonding state and empty antibonding states, obtained from the coupling of the dangling bonds, as is the case for example on Si(100)(2×1).[32] The instability suggested by the presence of half-filled dangling bonds bands, which induces a large peak in the surface projected density of states (SDOS) at E_F, is removed instead in surface C. Not surprisingly, unsaturated dangling bonds at E_F are absent in surface C, where, instead, one can recognize (see Fig. 4) surface states in three energy regions: (i) surface states near Γ just above and below the Fermi level, (ii) surface states 5 eV below E_F near the C point, and (iii) surface states in the surface-projected bulk gap 7–8 eV below E_F extending almost throughout the BZ in Fig. 4. These states show up very clearly in Fig. 7, where the SDOS is compared to the DOS projected in the center layer of the slab (bulk DOS). The surface-state contributions to the SDOS are indicated as shaded areas in Fig. 7. The pseudogap at E_F in the bulk DOS is largely smoothed in the SDOS of surface C, which is now much more similar to the SDOS of epitaxial GaIII than to the α-Ga bulk DOS, as we can see in Fig. 7. However, a remnant of the α-Ga pseudogap is still present in the SDOS of surface C; the two large peaks just above and below E_F in SDOS of surface C do not completely fill the pseudogap. The peaks in the SDOS of surface C just below and above E_F are produced from states (mainly

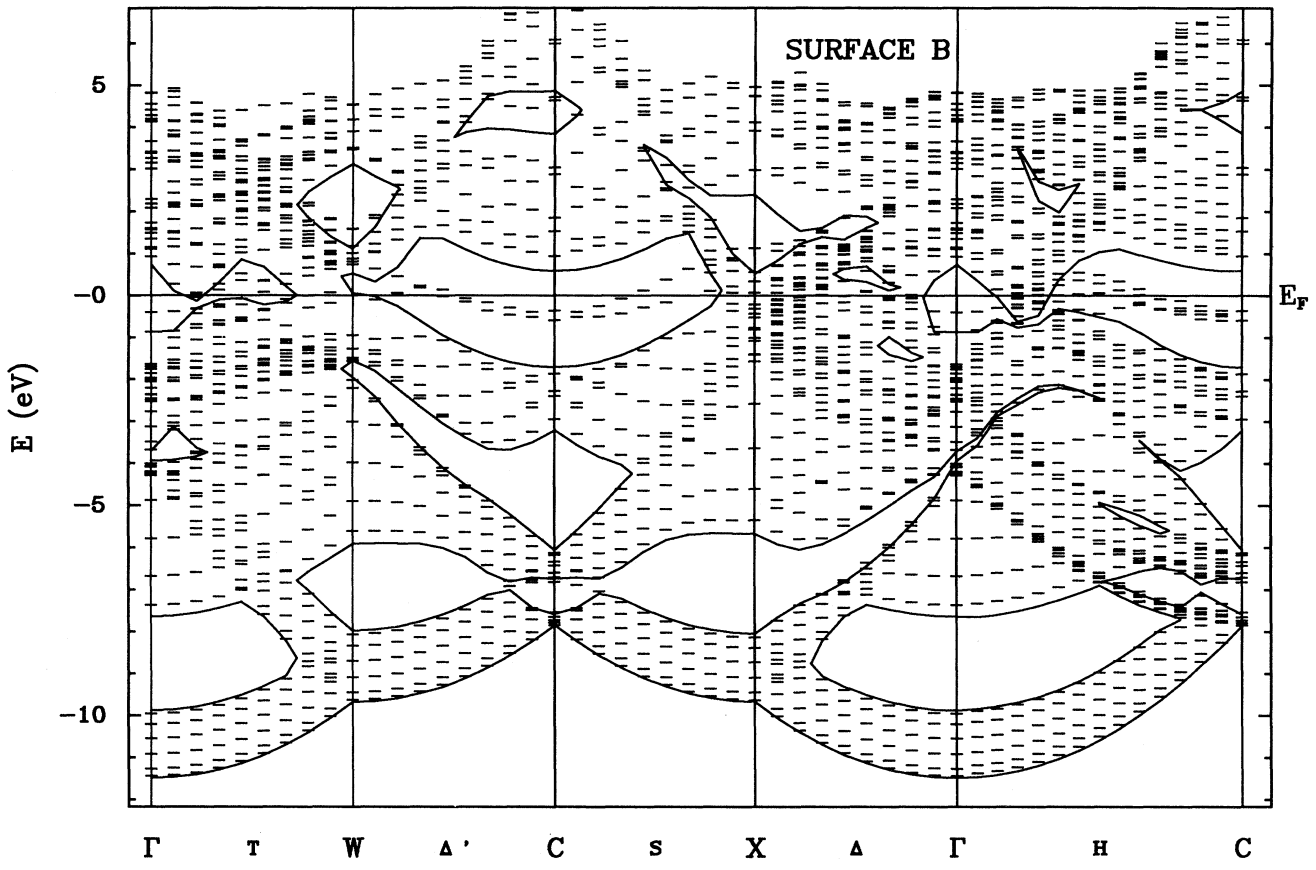

FIG. 5. The same as in Fig. 4 for surface *B*. The slab is 12 layers thick. The difference in the number of electronic states per k point in Figs. 4 and 5 is due to different slab thicknesses. Note the surface states crossing the Fermi level ("dangling bonds" states) and their absence in surface *C*, (Fig. 4).

near Γ point) extending throughout the GaIII film.

The surface states 4–5 eV below E_F (cf. Fig. 4) in surface *C*, give a large contribution to the bond charge of the outermost dimer of α-Ga at the α-Ga/GaIII interface, as one clearly recognizes in Fig. 8. Conversely, the surface states in the range 7–8 eV below E_F are localized mainly on the outermost plane midway the two surface atoms along the [100] direction. A representative state is shown in Fig. 9. Note also that the peak in the bulk DOS around 2 eV below E_F, which gives the maximum contribution to the bond charge of the dimers in the bulk α-Ga, is strongly smoothed in the SDOS of surface *C* in Fig. 7, as a further indication of the disappearance in the GaIII film of the covalent bonds typical of α-Ga.

Summarizing, we have seen that the presence of the GaIII film induces a large increase in the SDOS near E_F, which becomes smoother and more metallic, similar to that of GaIII. This metallization of the surface should, in principle show up in photoemission measurements. The detection of surfaces states at 7–8 eV below the Fermi level in the whole SBZ in angle-resolved photoemission, should be a further signature of surface *C*. Furthermore, the residual pseudogap in the SDOS of surface *C* is sufficiently small to account for the structureless *I-V* spectra recorded with STM by Züger and Dürig.[14]

IV. THE α-Ga(010) SURFACE

A. Surface structure

As reported, for instance, in Refs. 34 and 14, the (010) orientation is not present on α-Ga single crystals as grown from the melt. Instead, four small facets all belonging to the family of lattice planes indexed {121} are formed in the vicinity of the (010) orientation, and the (010) surface must be prepared by cutting the crystal. Its structure, expected from the truncated bulk, is shown in Fig. 10. The surface unit cell contains just one atom, the Ga_2 dimers being oriented out of the surface plane by an angle $\theta = 16.9°$, all in the same direction. An atomically resolved STM image of the (010) surface, recorded by Züger and Dürig,[14] is reproduced in Fig. 11. The best resolution of the image was obtained with tunneling parameters $I_t = 5$ nA, and $V_t = +50$ mV, i.e., by imaging empty electronic states of the sample. The symmetry ob-

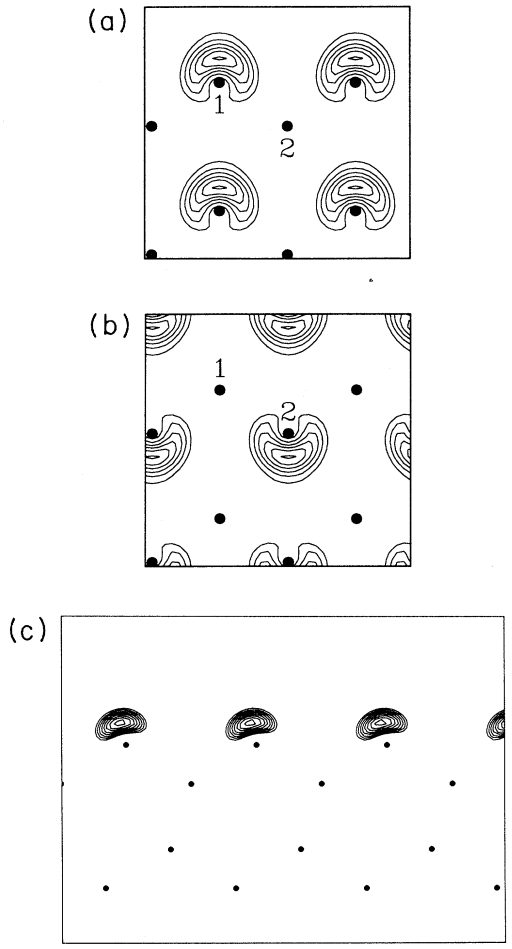

FIG. 6. (a) Charge density of a dangling bond state of surface B at $0.67k_{\Delta'}$, localized on atom 1 in the surface unit cell, plotted on the (001) plane. (b) The same as in (a) for the dangling bond localized on atom 2 in the surface unit cell. This eigenstate is degenerate in energy with the state in panel (a). (c) The eigenstate in panel (a) plotted on the (100) plane. Contour lines are separated by 0.0005 a.u.

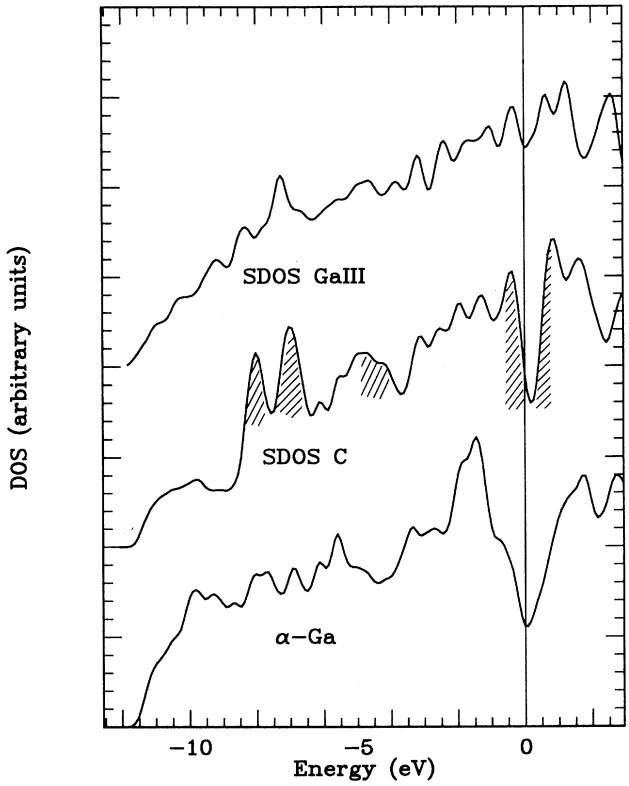

FIG. 7. The surface-projected DOS of surface C (14-layer slab), and of a relaxed 11-layer slab of epitaxial GaIII. The DOS projected on the center layer of the slab of α-Ga [bulk DOS (Ref. 10)] is also shown. The layer-resolved DOS's have been computed with the layer-projected KS orbitals from 49 k points uniformly spaced in the ISBZ. Band energies and projection integrals have been extended throughout the whole SBZ using the 2D version of the 3D tetrahedron method (Ref. 33). The resulting DOS has been further convoluted with a Gaussian with variance 80 meV. The SDOS of surface C is closer to the SDOS of epitaxial GaIII than to the bulk DOS of α-Ga.

served with STM is essentially in accordance with that expected from the truncated bulk in Fig. 10. However, Züger and Dürig recognized a slightly different contrast of the spots on the edges and in the center of the marked cells in Fig. 11 and suggested the possible occurrence of a 1×2 reconstruction. Although the absence of the (010) orientation in a single crystal suggests a high surface free energy $\gamma_{sv}^{(010)}$, large terraces extending over several hundred Å are present after sputter-cleaning cycles of the sample. Moreover, the step structure is stable up to T_m. Again, no dynamics such as roughening or diffusion at the steps edges was observed with STM up to the onset of bulk melting.[14] Thus, the (010) surface presents a thermal stability not unlike the (001) surface. These properties again suggest a possible self-wetting of the α-Ga(010) surface with a GaIII film. In particular, the geometry of the (010) surface might allow the epitaxial growth of a tetragonally distorted fcc film on top of α-

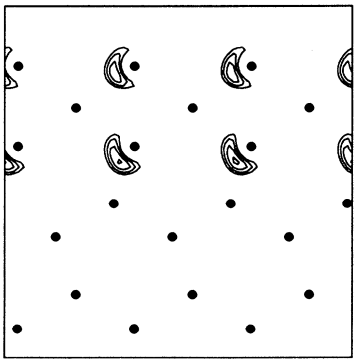

FIG. 8. Charge density plotted on the (100) plane of a surface state at C in the bulk-forbidden gap at -5 eV in Fig. 4. The maximum of the charge is localized in the bond of the outermost dimer of α-Ga at the α-Ga/GaIII interface. Contour lines are separated by 0.0002 a.u.

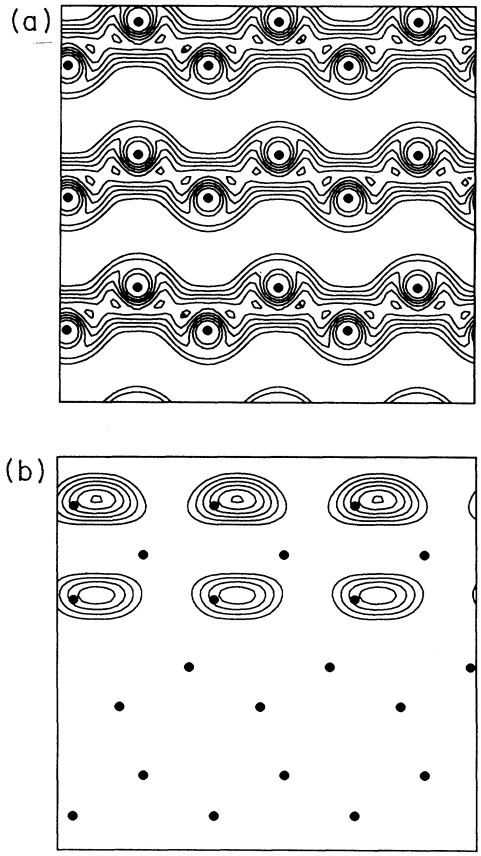

FIG. 9. Charge density of a surface state of surface C, belonging to the bands 8 eV below E_F at $0.22k_T$. (a) The (001) plane. (b) The (100) plane at $x=0.25$. The dots correspond to atoms lying on the (100) plane at $x=0$. Contour lines are separated by 0.0002 a.u.

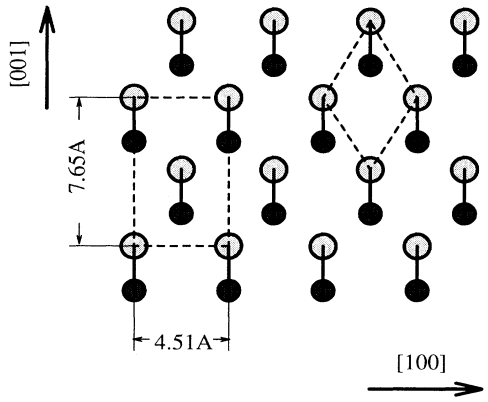

FIG. 10. Truncated bulk structure of the (010) surface. The Ga_2 dimers are oriented out of the surface plane by 16.9° (indicated by different shading). The ideal rhombohedral surface unit cell is depicted by dashed lines. The dashed rectangle denotes a conventional unit cell, twice as large as the ideal rhombohedral surface unit cell (Ref. 14).

Ga. However, the in-plane lattice constants are much larger on the (010) surface than on the (001) one. We found by a slab calculation that in this case, the large mismatch causes the GaIII film covering the (010) surface to be unstable with respect to the formation of dimers similar to those of bulk α-Ga. The final relaxed configuration of the slab presents a very large and unrealistic corrugation and a very high surface energy. Thus, self-wetting does not occur, and we have instead explored in more detail the properties of the ideal unreconstructed surface.

As for the (001) orientation, the ideal (010) surface can be formed in two ways: by cutting the crystal at a plane without cutting the dimers (surface A) or at a plane cutting the Ga_2 dimers (surface B). In configuration A three metallic bonds per atom are broken, while only two metallic bonds and one covalent bond per atom are broken in configuration B. On the basis of a simple bond strength and bond number argument, we, therefore, expect surface A to be favored. This is exactly what calculations confirm. We fully relaxed slabs 16–18 layers thick for both A and B geometries. The surface energies (γ_A) for the unrelaxed and relaxed A surface are found to be 97 and 79 mRy/atom, respectively. The difference between these (same orientation) is accurate with ± 1 mRy/atom. The absolute value of γ, however, is still somewhat slab dependent, mostly via the k-point mesh used for the computation of the bulk energy (E_{bulk}) to be subtracted from the total energy of the slab. By using E_{bulk} obtained from different k-point samplings, corresponding to 12-layer and 20-layer slabs, we obtain, for instance, a 7-mRy/atom difference in γ. The choice of the k-point mesh in the bulk BZ "equivalent" to the slab geometry is more critical for the (010) surface than for the (001) one because of the larger dispersion of electronic bulk bands along [010] than along [001] direction. We stress again that this uncertainty does not much affect the comparison of the surface energies of different slabs with the same orientation, but it does affect the analysis of the anisotropy of surface energy, i.e., for example, $\gamma^{(010)}-\gamma^{(001)}$. The above values for $\gamma^{(010)}$ refer to E_{bulk} calculated with a k-point mesh corresponding to a 12-layer slab. This choice corresponds to a 16-layer slab with the outermost dimer layers removed on both sides. The charge density on the (100) plane for surface A (18-layer slab) is shown in Fig. 12. Surface B is obtained by removing the outermost atom of the surface dimers in Fig. 12. The resulting surface has an exceedingly large corrugation. A better surface is obtained by moving the lone outermost atom in the hole underneath, midway the dimers of the second layer in Fig. 12. By fully relaxing this configuration, we ended up with a surface energy $\gamma_B=85$ mRy/atom, still higher than $\gamma_A=79$ mRy/atom. We finally conclude that the relaxed A surface in Fig. 12 is the *ground-state configuration* of the α-Ga(010) surface.

Note in Fig. 12 the decrease of the angle θ between the surface dimer and the surface plane from 16.9° down to 2.8°. The length of the surface dimer is basically equal to the bulk value. The dimer in the second layer is 1% contracted, and inclined by $\theta=15.4°$ ($\theta_{\text{bulk}}=16.9°$). A possible small difference of the angle θ of the two surface di-

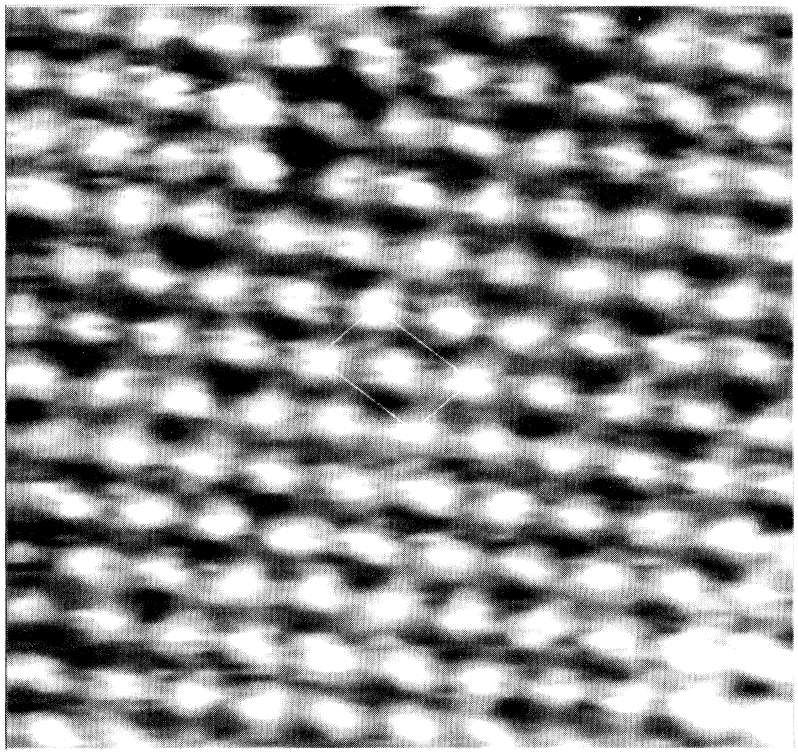

FIG. 11. Atomically resolved STM image (46×42 Å^2) of the (010) surface displaying $\partial \ln I_t/\partial x$ signal, (essentially $\partial z/\partial x$) measured by modulation technique (Ref. 14). The tunneling parameters are $I_t=5$ nA and $V_t=+50$ mV (positive voltage corresponds to imaging empty states of the sample). The corrugation calculated from this signal is 0.01 Å. The rectangular unit cells (cf. Fig. 10) are indicated by marked rectangles (slightly distorted by piezo shift). The figure is taken from Ref. 14 (courtesy of U. Dürig).

mers in the rectangular unit cell in Fig. 10 could be responsible for the asymmetry observed by STM,[14] but we have not explored this possibility further.

The rotation of the surface dimer reduces the charge corrugation and is responsible for the large energy gain obtained by relaxation. The two atoms of the surface dimer lie nearly on the surface plane, and the resulting atomic density of the relaxed (010) surface is 12.4 nm^{-2}, larger than that of the close-packed (001) surface (10.5 nm^{-2}). The (010) surface energy γ_A (4.9 mRy/Å^2) equals, within computational error, the surface energy of our proposed ground state for the (001) orientation (surface C in the preceding section). This result is perhaps not too surprising, in view of the similarity of atomic densities of surfaces (001) and (010). The absence of the (010) surface in the macroscopic shape of a single crystal grown from the melt might still be due to growth kinetics, which favor the other local minima in the polar plot of $\gamma_{sl}^{(hkl)}$, or perhaps to the nearby $\{121\}$ minima in the Wulff plot.

Although the surface dimer is nearly parallel to the surface, the innermost partner of the dimer is not visible in the theoretical STM image (cf. Fig. 14), in agreement with the experimental image in Fig. 11. Furthermore, the largest corrugation in the theoretical STM picture is obtained by imaging empty electronic states, again in agreement with experimental results.[14] This is clarified by examining the square amplitude of KS orbitals in the energy ranges $(-0.5,0)$ and $(0,+0.5)$ eV around E_F in Fig. 13. The protrusion of amplitude above the outermost atom in Fig. 13(a) is produced by a band of unoccupied surface states just above E_F (see Fig. 15 in the next section). In order to compute the STM image at the large experimental distances (5–8 Å) within the Tersoff-Hamann approximation, we have extrapolated the tails of the KS orbitals from ~ 3 Å outwards, by matching the KS orbitals of the slab calculation to the expected asymptotic decay, as described in the Appendix. The resulting theoretical STM image, nominally at 5 Å above the surface, is plotted in Fig. 14, including states inside an energy window 0.5 eV wide above (right panel) and below (left panel) E_F. In contrast to Fig. 13, 5 Å above the surface the maxima of charge density are always on top of the outermost atom of the dimer, imaging both empty and filled electronic states in Fig. 14. The image is thus expected to depend only weakly on the sign of tunneling voltage. The corrugation predicted by our calculations is 20–30 % larger by imaging empty states, in agreement with experiment. By further increasing the tip-surface separation above 8 Å, we predict that the largest corrugation should be obtained by imaging filled states. Moreover, in Fig. 14 the minima of the charge are along the [100] direction, midway between the maxima, while a saddle point is present along the [101] line connecting the maxima. This is precisely the behavior observed experimentally.[35]

B. Surface electronic properties

The slab electronic band structure of our best (010) surface configuration A is reported in Fig. 15. We recognize surface states in three energy regions: (i) empty surface states just above E_F near the bulk band edge along the T

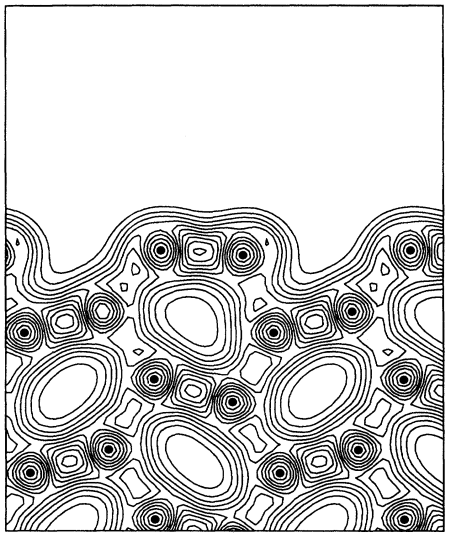

FIG. 12. Charge density of surface A [ground state of (010) orientation] plotted on the (100) plane passing through all atoms shown. Note the decrease of the angle between the outermost dimer and the surface plane. Contour lines are separated by 0.005 a.u.

direction, (ii) filled surface states in the small gap 3 eV below E_F, midway along T, and (iii) filled surface states 5–7 eV below E_F near Z. The charge density of representative surface states in the three energy regions (i), (ii), and (iii) is plotted in panels (a), (b), and (c) of Fig. 16, respectively. Surface states (i), just above E_F in Fig. 16(a), are strongly localized above the outermost atom and in the middle of the surface dimer bond. This surface band is responsible for the enhanced corrugation observed in STM by imaging empty states, as discussed in the preceding section. Surface state (ii), around 3 eV below E_F in Fig. 16(b), is localized between the second and third dimer layers, the distance between the two

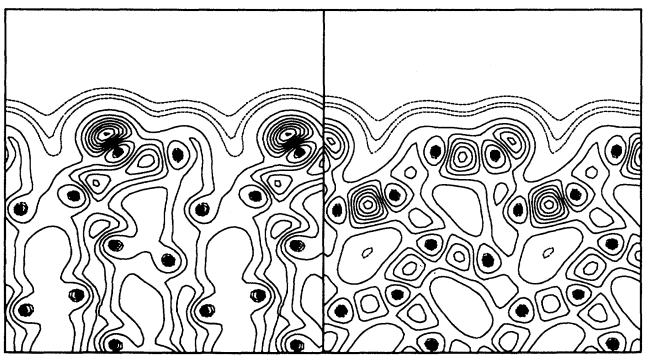

FIG. 13. Charge density of ground-state configuration of (010) surface plotted on the (100) plane, including states inside an energy window 0.5 eV wide above E_F (left panel) and below E_F (right panel). 52 k points uniformly spaced in the ISBZ are used. Continuous contour lines are separated by 3.8×10^{-4} a.u., while dashed lines are separated by 5.8×10^{-5} a.u., the lowest density being 5.8×10^{-5} a.u. The charge accumulation above the outermost atom in (a) is produced by empty surface states (cf. Fig. 15).

atoms "bonded" by the surface state in Fig. 16(b) being 5% lower than the corresponding bulk one. Surface state (iii) in Fig. 16(c), belonging to the surface band 5–7 eV below E_F, is strongly localized along the bond of the two outermost dimers. The surface states (i) and (iii), strongly localized on the surface dimers, show up clearly in Fig. 17 by comparing the SDOS with the DOS projected on the center layer of the slab. Surface states are indicated by shaded areas. We have found no indication of surface instability as produced, for instance, by half-filled surface states.

In summary, the configuration without broken dimers is favored on the (010) surface, as suggested by the simple counting of broken bonds. The resulting large corrugation, as well as the work function of the ideal bulk termination, is reduced by the rotation of the surface dimers. Such rotation is possible on the (010) surface, since all surface dimers are oriented in the same direction. On the contrary, on the (001) surface, in order to reduce corrugation, adjacent dimers should rotate in opposite directions. That rotation is hindered and will not occur, and the self-wetting scenario then prevails. These arguments rationalize the contrasting reconstructing and nonreconstructing behavior found on the (001) and (010) surfaces.

V. CONCLUSIONS AND OUTLOOKS

The uncertainty between two kinds of chemical bonds (metallic and covalent) gives gallium very peculiar properties. The partial covalent character of α-Ga and the closeness in energy of several other fully metallic phases[10] both play a role in the physics of α-Ga surfaces, where the relative importance of covalency and metallicity changes with respect to the bulk. We have proposed, based on detailed *ab-initio* calculations, that in the ground state the (001) surface of covalent α-Ga should, in fact, be covered with two layers of metallic GaIII grown epitaxially on α-Ga. GaIII is a denser phase stable in the bulk at high pressure and temperature. This realization of solid-state "self-wetting" phenomenon is made possible by the lower surface energy of GaIII, which makes it worthwhile paying for the difference in bulk energy between an α-Ga and a GaIII bilayer plus the interface energy. The cost of the GaIII film is indeed small because of the closeness in energy of the bulk phases, and the interface energy is reduced by the charge transfer across the α-Ga–GaIII interface connected with the 1-eV contact potential between the more electronegative α-Ga and more metallic GaIII. The metallization of the surface has been tentatively suggested also to be the source of the strong attraction between the GaIII/vacuum surface and the α-Ga/GaIII interface.[17] Consistently with experimental step distribution, this limits the GaIII film to strictly two atomic layers, with an incomplete wetting of α-Ga by epitaxial GaIII.

The theoretical STM image of our proposed ground state compares qualitatively well with the experiment. The presence of the metallic overlayer should be easily detectable by standard structural tools such as ion scattering, dynamical LEED, and x-ray diffraction. In

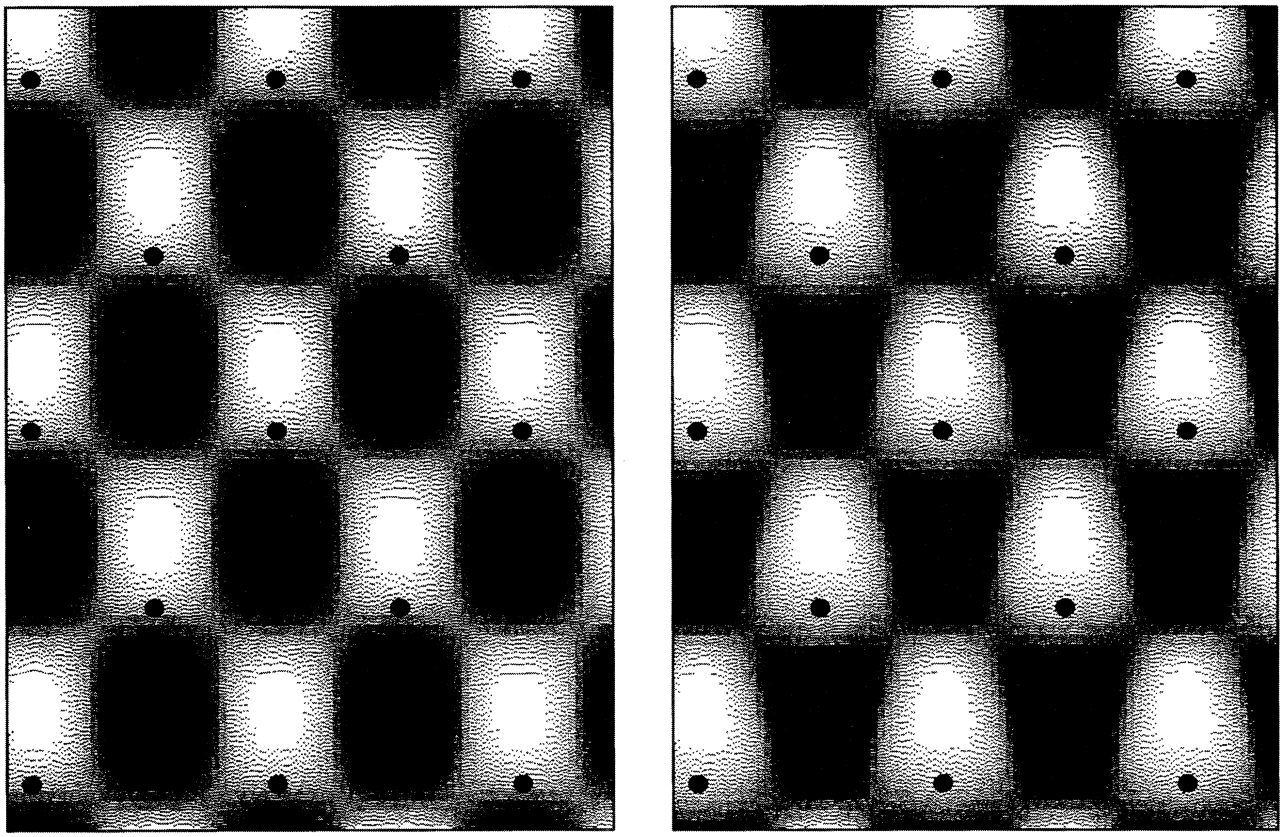

FIG. 14. Theoretical STM image for fixed 5-Å tip-surface separation, obtained by the extrapolation of KS orbitals tails, including states inside an energy window 0.5-eV wide above E_F (left panel) and below E_F (right panel). 52 k points uniformly spaced in the ISBZ are used. The matching point between KS orbitals of the slab calculation, and their expected asymptotic decay (see the Appendix) is 1.3 Å above the surface. The image with a matching point 3 Å above the surface is not noticeably different. Black dots indicate the outermost atoms of the dimers, while the innermost atoms are invisible in the dark regions.

this paper we have reported the detailed electronic band structure, which could be studied by angle-resolved photoemission, possibly providing a further check for our prediction.

Bulk GaIII is expected to melt above the melting point of α-Ga at the density of the film covering the α-Ga (001) surface. This argument could also explain the anomalous thermal stability of the (001) surface detected with STM. Although there is now experimental[36] and theoretical[37] evidence on the possibility of superheating closed packed surfaces [e.g., Au(111) and Pb(111)], the α-Ga(001) surface presents a more pronounced stability. In STM measurements[14] this face appears stable even when large amounts of the underlying bulk Ga are already melted. Our self-wetting scenario may therefore account for the enhanced thermal stability of α-Ga(001).

It has been noted that most of the other surfaces studied by STM [$\langle 001 \rangle$, (111), and (110)] also present a very low mobility up to T_m (303 K). The low diffusion at room temperature could be accounted for by considering that although the melting point of α-Ga is much lower than in most of other metals, the potential barriers to be overcome for adatom diffusion and/or the energy for the creation of a vacancy/adatom pair are probably not so much lower. An *ab-initio* study of the energy barriers for adatom diffusion would be quite illuminating in this respect. In particular, the reasons that instead, give rise to higher mobility observed on (112) remain to be clarified.

In contrast with the (001) orientation, the (010) surface does not metallize. We propose that on the (010) surface the Ga_2 dimers simply undergo a minor rearrangement consisting of a 14° rotation of the surface dimers, which reduces corrugation and minimizes the energy.

In summary our study reveals interesting phenomena at the surfaces of α-Ga driven by the interplay between covalency and metallicity. We hope that these results will stimulate further experimental work on this peculiar system.

ACKNOWLEDGMENTS

We are deeply indebted to Dr. U. Dürig and Dr. O. Züger for discussions and for providing us with the STM data reported in this paper, and to S. Baroni, M. Buongiorno Nardelli, A. Dal Corso, and P. Giannozzi for pro-

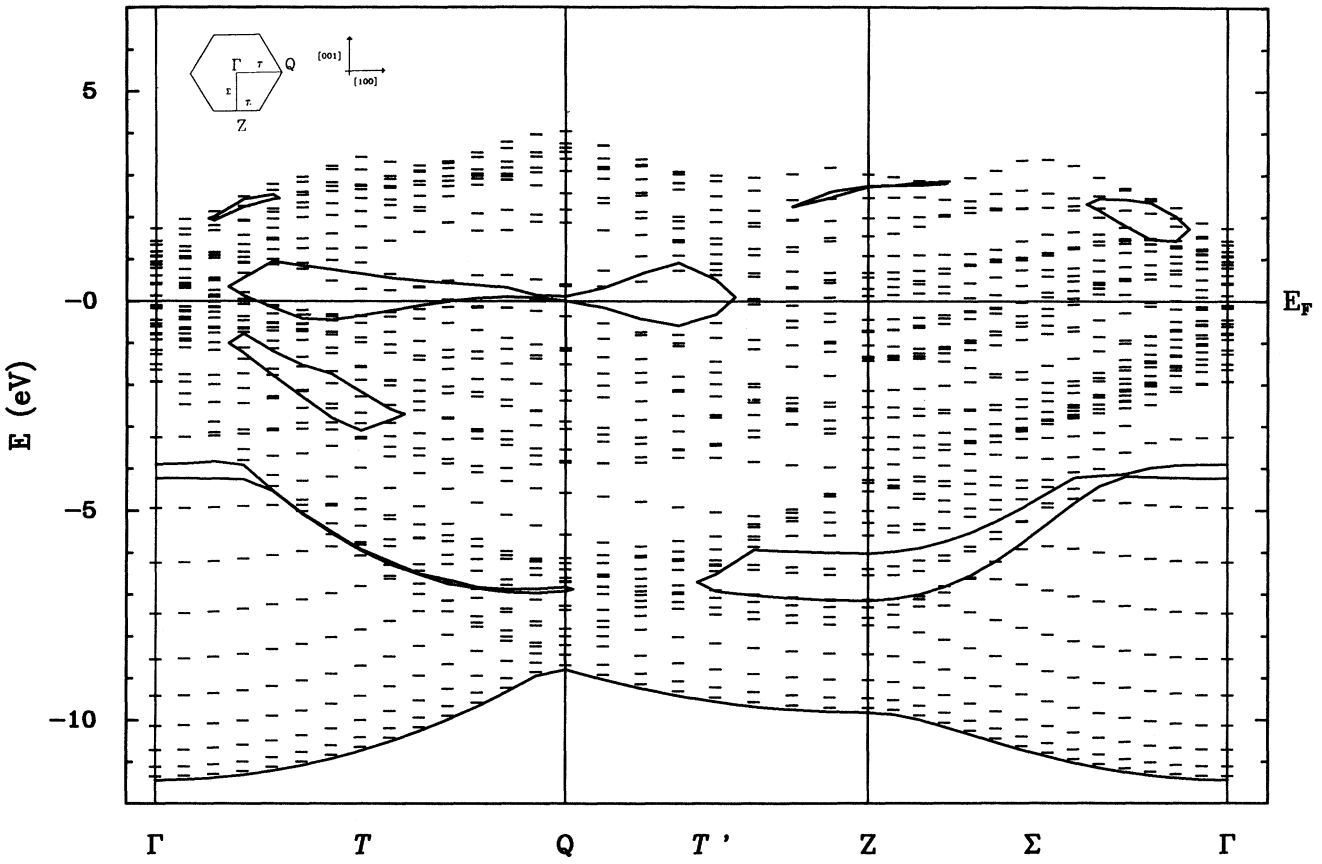

FIG. 15. The surface band structure of (010) surface (cf. Fig. 12) from a 18-layer slab. Continuous lines represent the band edges of the surface projected band structure of the bulk. The zero in energy corresponds to the Fermi level. The energies of bulk and slab calculations are aligned by matching the average Hartree potential in the bulk and at the center of the slab. Inset: Irreducible surface Brillouin zone for the (010) surface.

viding us with their DFT Fortran library. This work was supported by the Italian Consiglio Nazionale delle Ricerche through Progetto Finalizzato Sistemi Informatici e Calcolo Parallelo and SUPALTTEMP, by INFM, and by EEC, through Contract Nos. ERBCHBGCT920180 and 940636, as well as ERBCHRXCT930342.

APPENDIX: CALCULATED STM IMAGE

The simple first-order theory applied to tunneling by Bardeen[38] was specified to tip-surface tunneling by Tersoff and Hamann.[39] In this approximation, assuming a spherical tip with an s-wave function and featureless density of states, and with other reservations discussed in detail, e.g., in a recent review article,[40] the differential tunneling conductance is simply proportional to the surface DOS at the Fermi level measured at the tip center $\mathbf{r}_0$,

$$\frac{dI}{dV} \sim A\rho(\mathbf{r}_0, E=E_f) = A\sum_{n\mathbf{k}} |\psi_{n\mathbf{k}}(\mathbf{r}_0)|^2 \delta(E_{n\mathbf{k}} - E_f) \ , \quad \text{(A1)}$$

the constant A depending on the radius, work function, and DOS of the tip. For small tunneling voltage,

$$I \sim \rho(\mathbf{r}_0, E=E_f)V \ , \quad \text{(A2)}$$

so the variation in the current intensity at constant voltage and surface-tip separation reflects the variation of the local charge density, which can be used as a surface topograph to the extent to which the wave function at the Fermi level are sufficiently representative of the full set of occupied states. This may be the case in a regular metal, but it is clearly not so in a semimetal, and even less in a semiconductor.[40,41]

Expression (A2) is used for our calculations of the theoretical STM images. The typical tip-surface separation in experimental devices is of the order of 5–8 Å, so the wave functions should be evaluated very far from the surface in order to compare with experimental results. On the other hand, in a slab calculation the wave functions are only well described close to the surface because of the finite thickness of the vacuum region (9 Å in our case) and to the low cutoff energy, which cannot describe the exponential decay far from the surface. By plotting the logarithm of the charge density as a function of the distance from the surface, we recognized a good exponential decay of our wave functions up to 3 Å from the sur-

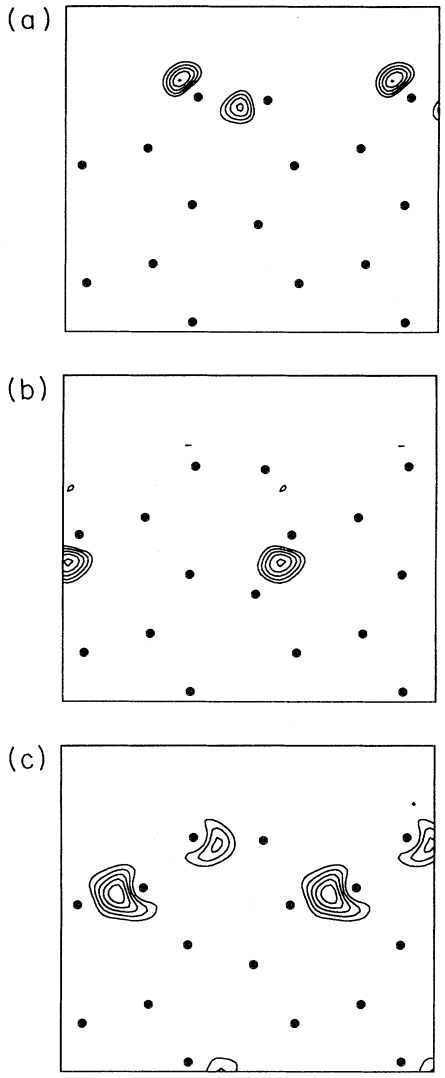

FIG. 16. Charge density plots of (a) the state at $0.5k_T$ of the surface band just above E_F, (b) the state at $0.5k_T$ of the surface band 3 eV below E_F, and (c) the state at $0.83k_\Sigma$ of the surface band 5–7 eV below E_F. Contour lines are separated by 0.0005 a.u.

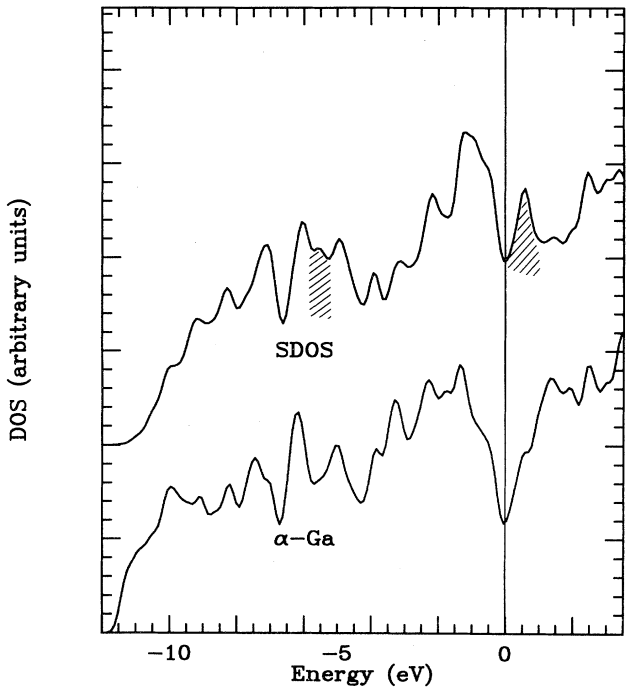

FIG. 17. Layer-projected DOS for (010) surface (18-layer slab). The upper curve is the DOS projected on the surface layer, while the lower curve is the DOS projected on the center layer of the slab. The layer-resolved DOS have been computed with the layer-projected KS orbitals from 52 k points uniformly spaced in the ISBZ. Band energies and projection integrals have been extended throughout the whole SBZ using the 2D version of the 3D tetrahedron method (Ref. 33). The DOS projected on the center layer of the (001) oriented slab reproduces better the bulk DOS (Refs. 6 and 10 and Fig. 7) than the bulk-projected DOS reported in this figure, due to a larger dispersion of the bulk bands along the [010] direction than along the [001] direction.

face. However, the exact form of the wave functions tail far from the surface is known as[39]

$$\psi_{n\mathbf{k}}(\mathbf{r})=\Omega^{-1/2}\sum_{\mathbf{G}} a_{\mathbf{G}} e^{-(\kappa^2+|\kappa_{\mathbf{G}}|^2)^{1/2}z} e^{i\kappa_G \mathbf{x}}, \tag{A3}$$

where $\mathbf{x}$ lies in the plane parallel to the surface, and z is perpendicular to the surface: $\kappa=2\pi/h\,(2m\phi)^{1/2}$, ϕ is the work function, $\kappa_G=\mathbf{G}+\mathbf{k}_{\|}$, and $\mathbf{G}$ is a surface reciprocal lattice vector. The $\psi_{n\mathbf{k}}$ obtained from the solution of the KS equation in reciprocal space reads

$$\psi_{n\mathbf{k}}(\mathbf{r})=\Omega^{-1/2}\sum_{\mathbf{G},g_z} b_{\mathbf{G},g_z} e^{ig_z z} e^{i\kappa_G \mathbf{x}}, \tag{A4}$$

where $(\mathbf{G},g_z)$ are the reciprocal lattice vectors of the 3D supercell. By equating Eqs. (A3) and (A4) at a point z_0 far from the surface, where ψ is well described by (A4), and hopefully also by (A3), we obtain the coefficient $a_{\mathbf{G}}$ in (A3) , which lets us evaluate the STM image at a point z arbitrarily far from the surface. For z in the range 5–8 Å, our STM images are not much dependent on the position of the matching plane z_0 at a distance from surface varying in the range 1.5–3 Å. Because of the use of a coarse mesh in the SBZ, we included in the sum over $n,\mathbf{k}$ in Eq. (A1), states inside an energy window 0.5 eV in size, below or above the Fermi level depending on the sign of the experimental tunneling voltage to be compared with. The work function in Eq. (A3) is consequently modified as $\phi\rightarrow\phi-[E_{n,\mathbf{k}}-(E_f+0.5\text{ eV})]$ by imaging empty states, and $\phi\rightarrow\phi-(E_{n,\mathbf{k}}-E_f)$ by imaging filled states.

*Present address: Max Planck Institut für Festkörperforschung, Postfach 8006565, Stuttgart, D-70506 Germany.

[1]R. W. G. Wyckoff, *Crystal Structures,* 2nd ed. (Wiley, New York, 1962), Vol. I, p. 22. A word of caution is in order: of the six possible ways to assign a,b,c to the three crystal axes, at least three different versions can be found in the literature.

[2]L. Bosio, J. Chem. Phys. **68**, 1221 (1978).

[3]L. Bosio, A. Defrain, H. Curien, and A. Rimsky, Acta Crystallogr. B **25**, 995 (1969).

[4]L. Bosio, H. Curien, M. Dupont, and A. Rimsky, Acta Crystallogr. B **28**, 1974 (1972).

[5]L. Bosio, H. Curien, M. Dupont, and A. Rimsky, Acta Crystallogr. B **29**, 367 (1973).

[6]X. G. Gong, G. L. Chiarotti, M. Parrinello, and E. Tosatti, Phys. Rev. B **43**, 14 277 (1991).

[7]V. Heine, J. Phys. C **1**, 222 (1968).

[8]J. E. Inglesfield, J. Phys. C **1**, 1337 (1968).

[9]J. Hafner and W. Jank, Phys. Rev. B **42**, 11 530 (1990).

[10]M. Bernasconi, G. L. Chiarotti, and E. Tosatti, preceding paper, Phys. Rev. B **52**, 9988 (1995).

[11]A. Dal Corso and E. Tosatti, Phys. Rev. B **47**, 9742 (1993).

[12]See, e.g., E. Tosatti, in *The Structure of Surfaces II,* edited by J. F. Van der Veen and M. A. Van Hove (Springer-Verlag, Berlin, 1988), p. 535.

[13]O. Züger and U. Dürig, Phys. Rev. B **46**, 7319 (1992).

[14]O. Züger, Ph.D. thesis, Eidgenössische Technishe Hochschule, Zürich, 1992; O. Züger and U. Dürig, Ultramicrosc. **42**, 520 (1992).

[15]An exception appears to be the (121) surface, see R. Trittibach, Ch. Grütter, and J. H. Bilgram, Phys. Rev. B **50**, 2529 (1994).

[16]M. Bernasconi, G. L. Chiarotti, and E. Tosatti, Phys. Rev. Lett. **70**, 3295 (1993).

[17]M. Bernasconi, G. L. Chiarotti, and E. Tosatti, Surf. Sci. **307**, 936 (1994).

[18]J. P. Perdew and A. Zunger, Phys. Rev. B **23**, 5048 (1981).

[19]L. Kleinman and D. M. Bylander, Phys. Rev. Lett. **48**, 1425 (1982).

[20]R. Stumpf, X. Gonze, and M. Scheffler (unpublished).

[21]R. P. Feynman, Phys. Rev. **56**, 340 (1939).

[22]O. H. Nielsen and R. M. Martin, Phys. Rev. B **32**, 3780 (1985); **32**, 3792 (1985).

[23]M. Methfessel and A. T. Paxton, Phys. Rev. B **40**, 3616 (1989).

[24]C. L. Fu and K. M. Ho, Phys. Rev. B **28**, 5480 (1983).

[25]P. Gomes Dacosta, O. H. Nielsen, and K. Kunc, J. Phys. C **19**, 3163 (1986).

[26]Perhaps the interatomic distances along the chains in the [100] direction are too small to favor the dimerization because of a 3% error in the theoretical lattice constant (Ref. 10). We indeed found, in a forcibly dimerized configuration of surface C, that by artificially expanding (contracting) the lattice parameter by 3% with respect to the theoretical equilibrium value, the forces that act to remove the dimerization undergo a 35% reduction (43% increment). A full relaxation of the dimerized configuration with expanded lattice parameters ends up with a still undimerized chain, because perhaps of the larger compression of the outermost layer induced by the artificial in-plane expansion.

[27]The distance along the [010] direction of the two surface atoms in the unit cell are 0.319 and 0.321 (in units of $a=4.38$ Å) for the epitaxial GaIII surface and surface C, respectively. For bulk epitaxial GaIII the same quantity is 0.358, i.e., the chains along the [100] direction in epitaxial GaIII are more packed at the surface than in the bulk.

[28]Because of a misprint, the stress tensor values, reported in Ref. 16 are incorrect and should be replaced by the present ones.

[29]γ_4 is obtained from a fully relaxed slab, 12 layers thick, where one surface has the geometry of configuration C and the other is covered with four layers of GaIII.

[30]The estimate of the melting temperature of GaIII was obtained by linear extrapolation of the experimental liquid-GaIII coexistence line in Ref. 2 up to the pressure needed to induce an 8% density increase of bulk GaIII at 0 K.

[31]The dangling bonds repel each other also in the configuration obtained by moving atom 2 in Fig. 6 in the specular position with respect to the [010] plane.

[32]N. Roberts and N. J. Needs, Surf. Sci. **236**, 112 (1990); J. A. Appelbaum, G. A. Baraff, and D. R. Hamann, Phys. Rev. B **14**, 588 (1976).

[33]O. Jepsen and O. K. Andersen, Solid State Commun. **9**, 1763 (1971); H. L. Skriver, *The LMTO Method* (Springer-Verlag, Berlin, 1984), p. 194.

[34]R. Kofman, P. Cheyssac, and J. Richard, Phys. Rev. B **16**, 5216 (1977).

[35]U. Dürig (private communication).

[36]J. W. Herman and H. E. Elsayed-Ali, Phys. Rev. Lett. **68**, 2952 (1992); **68**, 1228 (1992); E. A. Murphy, H. E. Elsayed-Ali, and J. W. Herman, Phys. Rev. B **48**, 4921 (1993).

[37]P. Carnevali, E. Ercolessi, and E. Tosatti, Phys. Rev. B **36**, 6701 (1987); H. Häkkinen and U. Landman, Phys. Rev. Lett. **71**, 1023 (1993).

[38]J. Bardeen, Phys. Rev. Lett. **6**, 57 (1961).

[39]J. Tersoff and D. R. Hamann, Phys. Rev. B **31**, 805 (1985).

[40]J. Tersoff, in *Scanning Tunneling Microscopy and Related Methods,* edited by R. J. Behm, N. Garcia, and H. Rohrer (Kluwer Academic, Dordrecht, 1990), p. 77.

[41]A. Selloni, P. Carnevali, E. Tosatti, and C. D. Chen, Phys. Rev. B **31**, 2602 (1985).

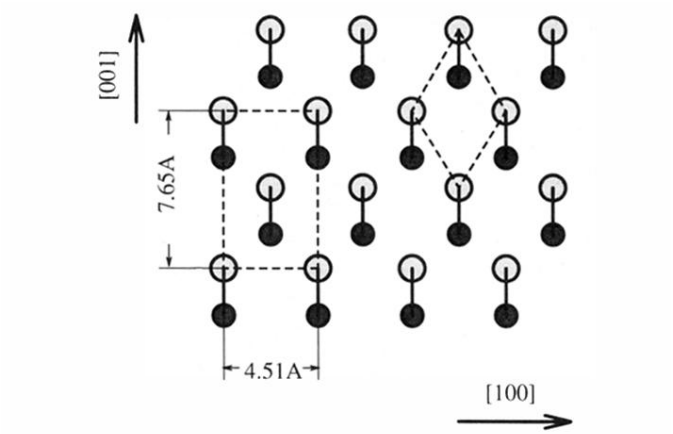

FIG. 10. Truncated bulk structure of the (010) surface. The Ga_2 dimers are oriented out of the surface plane by 16.9° (indicated by different shading). The ideal rhombohedral surface unit cell is depicted by dashed lines. The dashed rectangle denotes a conventional unit cell, twice as large as the ideal rhombohedral surface unit cell (Ref. 14).

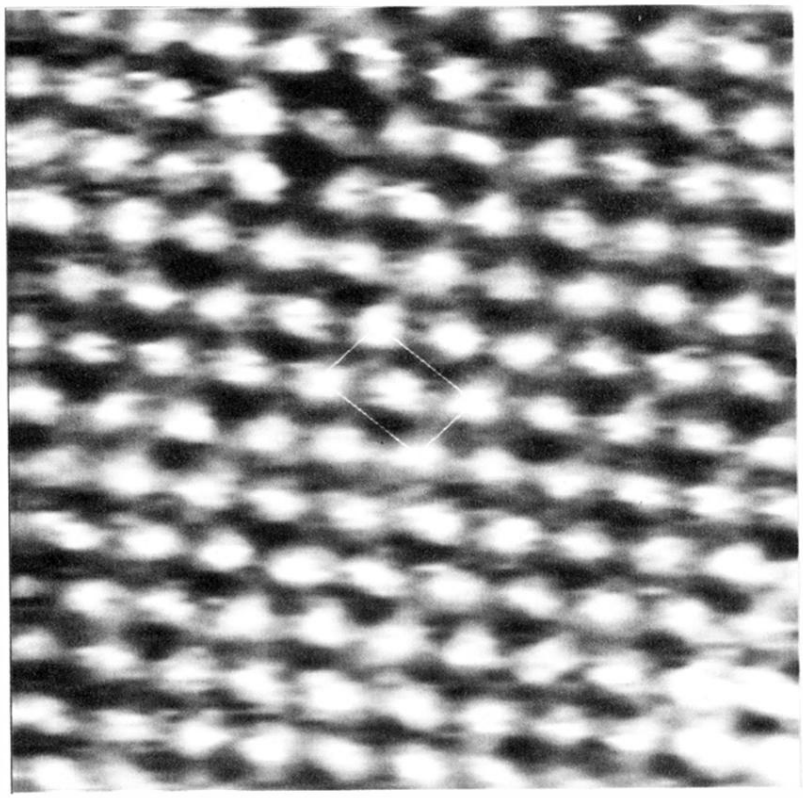

FIG. 11. Atomically resolved STM image (46×42 Å^2) of the (010) surface displaying $\partial \ln I_t / \partial x$ signal, (essentially $\partial z / \partial x$) measured by modulation technique (Ref. 14). The tunneling parameters are $I_t = 5$ nA and $V_t = +50$ mV (positive voltage corresponds to imaging empty states of the sample). The corrugation calculated from this signal is 0.01 Å. The rectangular unit cells (cf. Fig. 10) are indicated by marked rectangles (slightly distorted by piezo shift). The figure is taken from Ref. 14 (courtesy of U. Dürig).

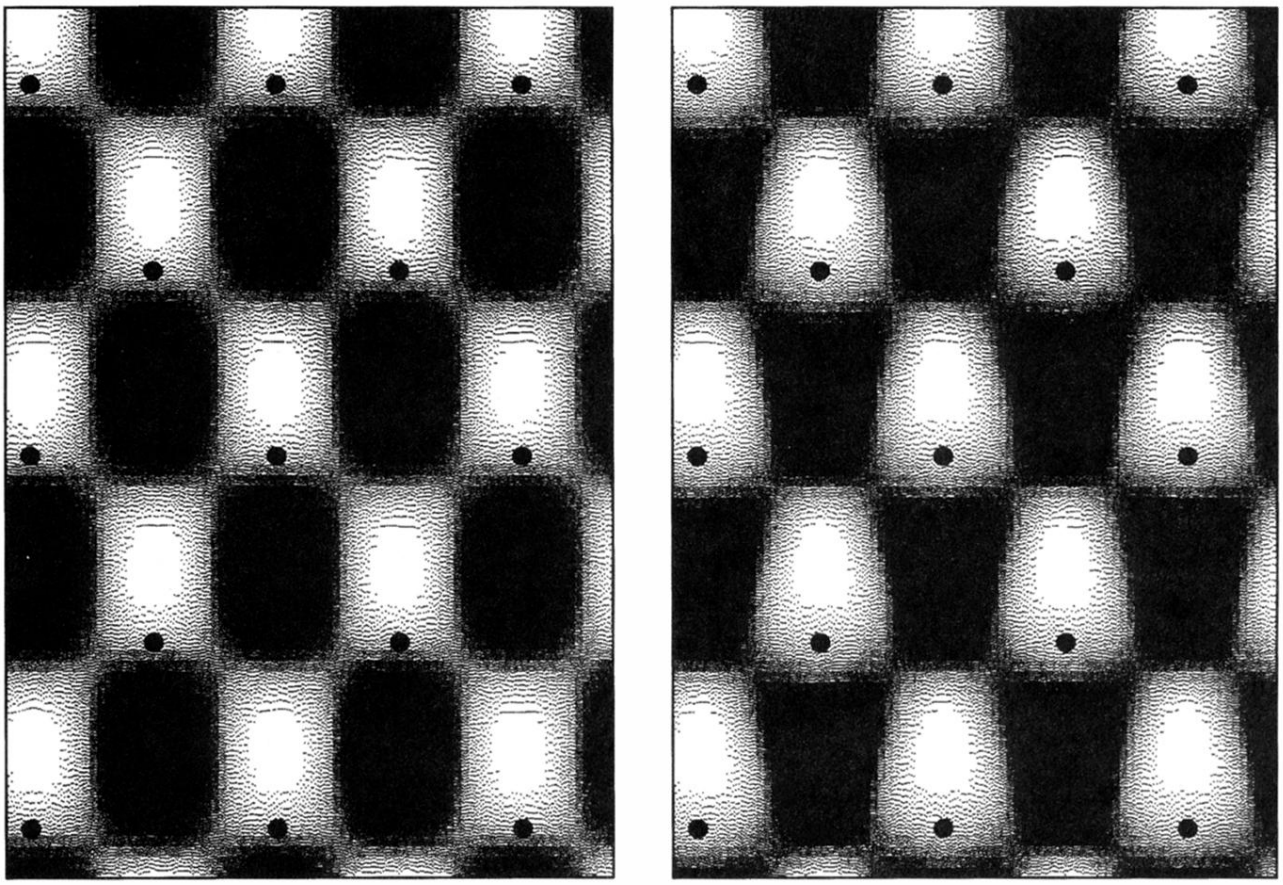

FIG. 14. Theoretical STM image for fixed 5-Å tip-surface separation, obtained by the extrapolation of KS orbitals tails, including states inside an energy window 0.5-eV wide above E_F (left panel) and below E_F (right panel). 52 k points uniformly spaced in the ISBZ are used. The matching point between KS orbitals of the slab calculation, and their expected asymptotic decay (see the Appendix) is 1.3 Å above the surface. The image with a matching point 3 Å above the surface is not noticeably different. Black dots indicate the outermost atoms of the dimers, while the innermost atoms are invisible in the dark regions.